Journal of Materials Chemistry C

Accepted Manuscript

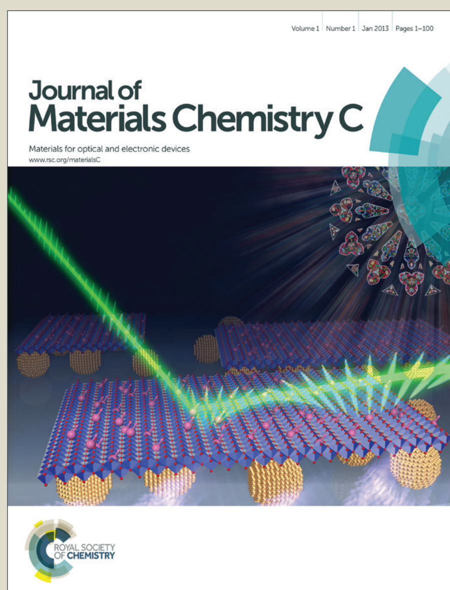

This is an *Accepted Manuscript*, which has been through the Royal Society of Chemistry peer review process and has been accepted for publication.

Accepted Manuscripts are published online shortly after acceptance, before technical editing, formatting and proof reading. Using this free service, authors can make their results available to the community, in citable form, before we publish the edited article. We will replace this *Accepted Manuscript* with the edited and formatted *Advance Article* as soon as it is available.

You can find more information about *Accepted Manuscripts* in the Information for Authors.

Please note that technical editing may introduce minor changes to the text and/or graphics, which may alter content. The journal's standard Terms & Conditions and the Ethical guidelines still apply. In no event shall the Royal Society of Chemistry be held responsible for any errors or omissions in this *Accepted Manuscript* or any consequences arising from the use of any information it contains.

ROYAL SOCIETY OF CHEMISTRY

www.rsc.org/materialsC

Interface control and modification of band alignment and electrical properties of HfTiO/GaAs gate stacks by nitrogen incorporation

Gang He[a,c*], Jiangwei Liu[b*], Hanshuang Chen[a], Yanmei Liu[a], Zhaoqi Sun[a], Xiaoshuang Chen[c] Mao Liu[d], and Lide Zhang[d]

[a]*School of Physics and Materials Science, Radiation Detection Materials & Devices Lab, Anhui University, Hefei 230039, P.R. China*

[b]*Optical and Electronic Materials Unit, National Institute for Materials Science (NIMS), 1-1 Namiki, Tsukuba, Ibaraki 305-0044, Japan.*

[c]*National Laboratory for Infrared Physics, Chinese Academy of Sciences, Shanghai Institute of Technical Physics, 500 Yutian Road, Shanghai 200083, P.R. China*

[d]*Key Laboratory of Materials Physics, Anhui Key Laboratory of Nanomaterials and Nanostructure, Institute of Solid State Physics, Chinese Academy of Sciences, Hefei 230031, P.R. China*

Email: hegang@ahu.edu.cn LIU.Jiangwei@nims.go.jp

Effect of nitrogen incorporation on the interface chemical bonding states, optical dielectric function, band alignment, and electrical properties of sputtering-derived HfTiO high-k gate dielectrics on GaAs substrate has been studied by angle resolved x-ray photoemission spectroscopy (ARXPS), spectroscopy ellipsometry (SE), and electrical measurements. XPS analysis has confirmed that the interfacial layer of HfTiO/GaAs gate stack has been suppressed effectively after nitrogen incorporation. Analysis from SE has confirmed that reduction in band gap and increase in refractive index has been observed with the incorporation of nitrogen. Reduction in valence band offset and increase in conduction band offset have been observed for HfTiON/GaAs gate stack. Electrical measurements based on metal-oxide-semiconductor (MOS)

Journal of Materials Chemistry C Accepted Manuscript

capacitors have shown that the MOS capacitor with HfTiON/GaAs stacked gate dielectric annealed at 600°C exhibits low interface-state density (2.8×10^{12} $cm^{-2}eV^{-1}$), small gate leakage current ($2.67\times10^{-5}Acm^{-2}$ at $Vg = V_{fb} + V$), and large dielectric constant (25.8). The involved mechanisms may originate from the decrease in the interface state density and the increase in the conduction band offset. The appropriate band offset relative to GaAs and excellent interface properties render HfTiON/GaAs promising gate stacks in future III-V-based devices.

INTRODUCTION

Metal-oxide-semiconductor field effect transistors (MOSFETs) with high-mobility channels such as III-V compound semiconductors are attracting an increasing interest as a solution for the saturation of the current drive and the performance of Si complementary metal-oxide-semiconductor (CMOS), particularly n-channel Si MOSFETs, which is a serious problems related to the scaling limit.[1-3] Among III-V compound semiconductors, GaAs has been investigated actively as an alternative channel material to Si for extending the performance limits of MOSFETs due to their significantly higher carrier mobility and smaller effective mass compared to those of Si or strained Si.[4] However, the absence of high quality MOS interface compared to that of SiO_2/Si interface retards the development of GaAs-based MOSFETs devices with high performance.[3,5,6] Therefore, for the successful realization of GaAs-based MOSFETs, there are still a number of fundamental issues to be solved.

One of the most critical challenges is the development of a high-quality and thermodynamically stable insulator on GaAs with a low density of interfacial trap states (D_{it}) or a good interfacial layer comparable to that of SiO_2/Si interface.[7] The high D_{it} associated with dielectric/GaAs interface causes Fermi level pinning at midgap, which inhibits formation of

Journal of Materials Chemistry C Accepted Manuscript

accumulation or inversion layers and degradation of the drive current and the sub-threshold swing.[8] The removal of surface species has been shown to be critical for unpinning the Fermi level.[9,10] As a result, control of the interfacial oxides on GaAs upon gate stack formation has been recently explored along different methods. Examples include deposition of a thin layer of Si or Ge as interfacial passivation layers, sulfide-based immersion, or nitridation pretreatment have been investigated and improvements in providing a high quality interface have also been demonstrated.[11-14] However, it can be noted that Si and Ge are amphoteric dopants for GaAs, a thin layer of Si or Ge may alter the doping concentration or even induce the counter doping of the GaAs substrate, causing the instability of the threshold voltage.[15] The reported D_{it} values of the sulfur-terminated GaAs MOS interface is about $10^{12}cm^2eV^{-1}$, which is much higher than that of SiO_2/Si MOS interface.[16,17] Fortunately, recent progress made in the direct deposition of new Hf-based high-k gate dielectrics due to its superior thermodynamic stability when in contact with the III-V substrate have reopened the possibility of realizing GaAs-based CMOS devices, overcoming its poor interface quality issues.[3,18] However, their moderate dielectric constants make Hf-based gate dielectrics limited for future CMOS device scaling with an EOT below 1.0 nm.[19] One of the effective ways to increase Hf-based dielectric permittivity is combining it with another much higher dielectric materials, such as TiO_2. Ti was added into Hf-based dielectrics to achieve a higher k value, remarkable thermal stability, and improved electrical properties have been reported.[20-22] Additionally, nitrogen incorporation has been reported to be an effective way to modulate the performance of some related devices.[23,24] Currently, nitrided HfTiO herein (designated as HfTiON) has also been extensively examined. Ji *et al*. have showed that NO-nitrided HfTiON gate dielectric MOS capacitor exhibits excellent electrical properties and reliability and gives a k value of 18.9.[25] It was shown by Li *et al*. that N incorporated into HfTiO

Journal of Materials Chemistry C Accepted Manuscript

can enhance its dielectric constant and reduce its oxide charges and border traps.[26] Our previous studies have also indicated that nitrogen-incorporation should improve electrical properties and interface quality of HfTiO thin films by cosputtering of Hf and Ti targets.[21,27] In spite of the improved thermal stability and electrical performance for III-V-based device, the pretreatment and the passivation of the surface layer prior to the Hf-based high-*k* gate dielectric deposition to minimize the oxides formation and eliminate the Fermi level pinning effect is still necessary,[11,28] which introduces more uncontrollable parameters and destroys the performance of the device. In current work, prior to the HfTiON gate dielectric deposition, except for chemical cleaning for GaAs substrate, no passivation layer is needed. By far, although there exist reported significant material improvements that nitridation enables, as noted above, the effect of nitrogen inclusion on the electronic structure of HfTiO without additional passivation layer, in general, and on the band alignments and electrical properties of HfTiON/GaAs gate stack in particular, has not been systematically investigated. In this letter, we focus on the investigation of interfacial chemical bonding state and depth profile of HfTiON/GaAs gate stack as a function of nitrogen content. Additionally, more attention has been paid to the evolution of the band offset, as well as the electrical properties of HfTiO and their nitrided derivatives.

EXPERIMENTAL

Commercially available *n*-type (100) GaAs wafers with doping concentration of (0.1~5) $\times 10^{18}$ cm^{-3} were chosen as the substrate. Prior to HfTiON gate dielectric deposition, the wafers were degreased using acetone and isopropnol, cleaned in HCl for native oxide removal, and dipped in NH_4OH for elemental As removal.[11]After cleaning, *ex-situ* HfTiON gate dielectrics with thickness of 2 nm confirmed by spectroscopy ellpsometry (SE) was deposited by sputtering equipment (JGP-DZS, Chinese Academy of Sciences, Shenyang Scientific Instrument Co., Ltd).

Journal of Materials Chemistry C Accepted Manuscript

The working pressure, deposition power, and deposition temperature were kept at 1.0 Pa, 100 W, and room temperature, respectively. Then radio frequency reactive sputtering of the HfTi alloy target was employed to deposit HfTiON thin films on the GaAs substrate with the $Ar/N_2/O_2$ mixture atmosphere. For comparison, HfTiO was also directly deposited on GaAs substrate without nitrogen incorporation. After the formation of various dielectric structures, the following characterizations were employed *ex-situ* for comparative study. The thickness and optical constant of the HfTiON and HfTiO films was obtained by spectroscopic ellipsometry (SE Model UVISEL JOBIN-YVON) analysis. To investigate the interfacial chemical bonding states and the valence band offset, *ex-situ* x-ray photoelectron spectroscopy (XPS) measurements were performed by using (ESCALAB 250Xi) system, equipped with an Mg Kα radiation source (1253.6 eV). For the depth profiling of different atoms in gate stack, an emission angle from samples surface normal setup was changed from 0° (bulk sensitive) to 80° (surface sensitive). The collected data were corrected for charging effect-induced peak shifts using the binding energy (BE) of adventitious carbon C 1*s* peak (284.6 eV). Spectral deconvolution was performed by Shirley background subtraction using a Voigt function convoluting the Gaussian and Lorentzian functions. In order to examine the electrical properties, MOS capacitors were fabricated by patterning the evaporation-deposited Au-capped top electrode via shadow mask method and Al was evaporated as the back electrode to decrease contact resistance, followed by forming-gas annealing at 400°C for 30 min under a flow of 5% H_2/N_2 mixed gas. The electrical characterization was performed at room temperature in a shielded dark box. High-frequency (1MHz) *C-V* characteristics were measured using an Agilent E4284A LCR meter. In addition, the leakage current characteristics were measured using a Keithley 4200 semiconductor device analyzer.

Journal of Materials Chemistry C Accepted Manuscript

Journal of Materials Chemistry C Accepted Manuscript

RESULTS AND DISCUSSION

Interface Bonding State Characteristics and Depth Profile

To investigate the effect of nitrogen incorporation on the chemical states of HfTiO gate dielectrics, Hf 4*f* and Ti 2*p* core-level spectra have been analyzed by XPS, as demonstrated in Fig. 1 and Fig. 2. Compared with the reported values of 16.2 and 17.8 eV for Hf $4f_{7/2}$ and Hf $4f_{5/2}$ peaks of HfO_2 as well as 458.3 and 464.3 eV for Ti $2p_{3/2}$ and Ti $2p_{1/2}$ peaks of TiO_2,[20,21] the binding energies corresponding to Hf 4*f* and Ti 2*p*, shown in Fig. 1(a) and Fig. 2(a), have no shift for HfTiO samples. Additionally, with the nitrogen incorporation into HfTiO, the Ti 2*p* peaks, shown in Fig. 2(b), still show no difference in chemical bonding state with that of HfTiO. However, the deconvoluted Hf 4*f* spectra of HfTiON sample, shown in Fig. 1(b), demonstrate a new feature. The binding energy of Hf $4f_{7/2}$ peaks located at 16.2 and 15.6 eV can be assigned to Hf $4f_{7/2}$ in HfO_2 and HfON phases, respectively.[29] The peak located at 15.6 eV may come from the Hf–O-N bond, demonstrating a 0.3 eV shift from the reported Hf–N bonding energy (15.3 eV) for $HfN_{1.9}$ films.[30] The peak located at 16.2 eV, attributed to Hf–O bond, also demonstrates shift from from our reported value.[31] The shift of binding energy of the Hf–O-N to a higher binding energy as well as the shift of Hf–O binding energy to a lower binding energy from the reported value indicate the presence of Hf–O bonds in addition to Hf–O-N bonds in the HfTiON films. Due to the photoelectron spectrum of Hf 4*f* overlapping that of Ga 3*d* spectrum, Fig. 1(a) also demonstrates some important information from HfTiO/GaAs interface. The peak at 20.4 eV originates from the Ga–O bond and another peak located at 18.8 eV is mainly attributed to the Ga–As bond from the GaAs substrate.[29] However, beside GaAs substrate, no additional peak corresponding to the Ga–O bond has been detected for HfTiON sample, shown in Fig. 1(b),

suggesting that the growth of the Ga oxide has been completely suppressed after nitrogen incorporation into HfTiO gate dielectric.

To further identify the effect of nitrogen incorporation on the interfacial chemical bonding state of HfTiO/GaAs gate stack more clearly, As 3*d* core-level spectra have been investigated, as shown in Fig. 3. For HfTiO sample, the As 3*d* spectra shown in Fig. 3(a), can be deconvoluted into two components at 41.3 and 44.3 eV corresponding to As–Ga and As–O, indicating that the formation of As–O bond has been detected.[29] However, for the nitrided sample, the HfTiON/GaAs is still found to be free from any GaAs oxides, suggesting that oxidation of GaAs surface is controlled effectively during nitrogen incorporation. To confirm our observation, the O 1s spectra (Fig. 4) also have been paid more attention. For the sample without nitrogen incorporation, the deconvoluted O1*s* spectra show four peaks, which are assigned as Hf-O, Ti-O, Ga-O, and As-O bonding states, respectively. However, for HfTiON/GaAs, shown in Fig. 4(b), no any oxide has been detected besides Hf-O and Ti-O components. Based on our observation, it can be concluded that the formation of oxides located at the interface region of HfTiO/GaAs gate stack has been suppressed effectively after nitrogen incorporation. Based on the observation from Ye,[32] Ti addition to HfO_2 only stabilizes the amorphous phase of HfO_2 and both HfO_2 and TiO_2 may exist as amorphous structure in the HfTiO composite and the atom cluster of them only simply mixes together. For nitrided samples, amorphous HfO_2 reacts with incorporated nitrogen and leads to the formation of HfON, which can act as an oxygen reaction barrier and minimize the formation of a low quality oxide.

In order to further confirm the evolution of the interfacial chemical bonding states related with nitrogen incorporation, the depth profile of HfTiO/GaAs gate stack has been investigated by angle resolved XPS (ARXPS) measurement, which is a non-destructive technique and has the

Journal of Materials Chemistry C Accepted Manuscript

Journal of Materials Chemistry C Accepted Manuscript

potential to probe subsurface chemical states. As we know, with the increase of emission angle, the probing depth becomes shallow and the surface region is probed. Therefore, by changing the emission angle, the information from the interfacial region will be detected. Fig. 5 and Fig. 6 show the 2D images of As 3*d*, Hf 4*f*, O 1*s*, and Ti 2*p* XPS spectra as a function of emission angle. For Ti 2*p* 2D images shown in Fig. 5(d) and Fig. 6(d), no apparent difference has been found regardless of nitrogen incorporation, indicating that the Ti 2*p* bonding states keep unchanged. For As 3*d* 2D images shown in Fig. 5(a), As-O and Ga-As bonding states have been detected in HfTiO/GaAs system. With the incorporation of nitrogen, only GaAs has been confirmed. Same trend has been observed in Hf 4*f* 2D images. With the increase in emission angle, the Ga-O and As-O bonding states still exist in HfTiO/GaAs gate stack, indicating that the oxide components are formed as reaction products in the more surface region near the HfTiO thin films. For O 1s 2D images shown in Fig. 5(c), the broadening of the O 1s XPS spectra for HfTiO sample indicating more components in HfTiO/GaAs gate stack. With the incorporation of nitrogen, the O 1s 2D image demonstrates narrowing trend, suggesting the reduction of component in HfTiON/GaAs gate stack. Based on ARXPS and 2D images for As 3*d*, Hf 4*f*, O 1*s*, and Ti 2*p* XPS spectra, it can be concluded that that the growth of the interface oxide has been completely suppressed with nitrogen incorporation, which is in good agreement with previous XPS observation.

Optical Constant Measurements

An ex-situ phase modulated SE (UVISEL Jobin-Yvon) was used to measure the optical functions of HfTiO and HfTiON films at room temperature in the spectral range 0.75-6.5eV with a step of 50 meV at an incident angle of 70°. The experimental parameters obtained by SE are the angles Ψ (azimuth) and Δ (phase change), which are related to the microstructure and optical properties,

defined by[21,33,34]

$$\rho = r_p/r_s = \tan\psi \exp(i\Delta)$$

Where r_p and r_s are the amplitude reflection coefficient for light polarized in the p- and s-planes of incidence, respectively. The spectral dependencies of ellipsometric parameters Ψ (azimuth) and Δ (phase change) can be fitted with appropriate models to extract film thickness and the optical constants, i.e., the refractive index (n) and extinction coefficient (k), based on the best fit between experimental and simulated spectra. For interpreting the measured pseudodielectric function, a four-layer-structured optical model consisting of GaAs substrates, the GaO_x interface layer, a bottom bulk HfTiON layer, and a surface rough layer composed of 50%void space and 50% HfTiON. In our SE analysis, Tauc-Lorentz (TL) dispersion function has been adopted to characterize the dielectric functions of the HfTiO and HfTiON films.[21] Essentially, the imaginary part (ε_2) of dielectric functions is obtained by combining the classical expression of the imaginary part of the dielectric functions above the band edge and the standard Lorentz expression, and the real part (ε_1) of dielectric functions is the result of self-consistent Kramers–Kronig integration of ε_2. The following equations summarize ε_1 and ε_2 as a function of photon energy E:

$$\varepsilon_2(E) = \begin{cases} \dfrac{AE_0C(E-E_g)^2}{(E^2-E_0{}^2)^2+C^2E^2}\cdot\dfrac{1}{E} & (E>E_g) \\ 0 & (E\leq E_g) \end{cases} \quad (1)$$

and $$\varepsilon_1(E) = \varepsilon_\infty + \frac{2P}{\pi}\oint \frac{\xi\varepsilon_2(\xi)}{\xi^2-E^2}d\xi \quad (2)$$

Journal of Materials Chemistry C Accepted Manuscript

Journal of Materials Chemistry C Accepted Manuscript

where E_0 is the resonance energy, E_g represents band gap energy, and A and C are the amplitude and broadening coefficient of the ε_2 peak, respectively. These are fitting parameters, together with the layer thickness in the least-squares fit procedure, which minimize the biased estimator x^2 defined as goodness-of-fit. Experimental (open and closed circles) and fitted (solid lines) spectra for the HfTiON films, together with the spectroscopic spectra of HfTiO, are shown in Fig. 7. It can be seen that the fitted spectra reproduce almost identically the experimental spectra in the entire measured photon energy range. Compared with HfTiO sample, the experimental spectra of the HfTiON samples demonstrate slight discrepancy, which can be attributed to the evolution of the morphologies and the change in the packing density after incorporation of nitrogen.[33] As is well known, morphologies will depolarize the detected polarizing light and affect the experimental ellipsometric parameters and lead to a deviation from each other. All these indicate that nitrogen incorporation has a significant effect on the optical properties.

By SE spectral analysis based on the accurately parameterized Taul–Lorentz dispersion relation for the HfTiO films,[21] the optical dielectric constants of the targeted films as a function of nitrogen content have been determined. Fig. 8(a) demonstrates the evolution of the refractive index (n) of HfTiO film related with nitrogen content. It can be noted that the increase of n after nitrogen incorporation can be due to the increase of packing density, which is in agreement with our previous observation for sputtering derived nitrogen-doped HfO_2 films.[35] Since metal–nitrogen bonds tend to be less polar than the corresponding metal–oxygen bonds leading to a higher polarizability for the metal nitride.[36] In our case, such a substitution in the anion lattice holds the promise to increase the refractive index. The energy dependence characteristic of indirect allowed transition as illustrated by the $(\alpha E)^{1/2}$ versus photon energy (E) plot is inserted in Fig. 8(a). Tauc plots indicate optical band gaps of 4.66 eV and 4.37 eV for the HfTiO and

Journal of Materials Chemistry C Accepted Manuscript

HfTiON, respectively.[21] It is obvious that reduction in band gap after nitridation has been observed, which originates from the N 2*p* level,[35] as explained below.

Fig. 8(b) shows the nitrogen content dependent real part (ε_1) of the optical dielectric constants ($\varepsilon=\varepsilon_1+i\varepsilon_2$) of HfTiO films as determined by SE. From Fig. 8, no shape change for ε_1 has been found regardless of the nitrogen incorporation. However, with nitrogen incorporation, it can be noted that ε_1 increases. It has been reported that the optical dielectric constants decreases with the increase of the band gap energy, which is due to the fact that the optical dielectric constant originating from electronic polarizability is strongly dependent on the width of the band gap energy, and is nearly independent of the origin of the band gap, i.e., the atomic composition.[37] This results suggests that the evolution of the optical dielectric constants is attributed to the change of the optical band gap with the nitrogen incorporation. Additionally, in the transparent region, the optical dielectric constant is similar to n^2 and it is related to the polarization. The increase of n indicates the increase of polarization and leads to the increased dielectric constant. The inset in Fig. 8(b) presents the spectra of the imaginary (ε_2) part of the dielectric functions for all the samples. Based on previous report,[37] the optical band gap can be obtained from the imaginary part of the dielectric constant. So the optical band gap values extracted from the imaginary part of the dielectric functions are 4.36 eV for HfTiON sample, and 4.66 eV for HfTiO, respectively. An apparent reduction in band gap after nitrogen incorporation in HfTiO has been observed, which is in good agreement with the previous observation. Similar phenomenon has been reported for N-doped HfO_2 films.[35] Based on Ye's observation,[32] in the case of HfTiO, nonbonding O 2*p* states form the top of the valence band (VB) and the antibonding 5*d*/3*d* states of Hf/Ti form the lowest conduction band (CB). In the case of HfTiON, incorporating N adds N 2*p* states which form the VB, which lie above the O 2*p* states in free

atoms, so the VB has been raised, the delocalized Hf/Ti *d*–N*p* bonding states leads to the reduction of band gap of HfTiO.[38]

Band Alignment and Electrical Characteristics

For better device scaling potential in terms of low gate leakage current, the dielectric layer is required to have sufficient barrier heights for both electron and hole injection. The monitored offsets in the valence-band spectra can be utilized to map out the energy-band alignment for the interface between HfTiO and GaAs substrate. According to the method proposed by Kraut *et al.*,[39] the valence band alignment of HfTiO films on GaAs substrate could be determined by measuring the valence band maximum (E_v) difference between the HfTiO films and the GaAs substrate, as expressed in the following equation:

$$\Delta E_v(\text{HfTiO} - \text{GaAs}) = E_v(\text{HfTiO}) - E_v(\text{GaAs}) \quad (1)$$

The E_v of each sample is determined by extrapolating the leading edge of valence band spectrum to the base line, the cross point is taken to be E_v,[40] as shown in Fig. 9. Fig. 9(a) shows the nitrogen-induced evolution of valence band offset (ΔE_v) of HfTiO/GaAs gate stack and reduction in ΔE_v has been detected after nitridation. Based on the corrected leading edge of valence-band spectra for native GaAs substrate, the valence-band offsets (ΔE_v) between the native GaAs substrates and HfTiO with/without nitridation, as highlighted in Fig. 9, are found to be 1.87 and 2.45 eV, respectively. As we know, the ΔE_v of HfTiO film is mainly determined by O 2*p* states which is similar to the case of TiO_2 and HfO_2,[21,35] while for the HfTiON thin films, it is necessary to consider the contribution of N 2*p* state which lies above that of the O 2*p* state, as a result, incorporation of N into HfTiO would reduce the ΔE_v of the films.

The conduction band offset (ΔE_c) can be obtained by simply subtracting the valence band offset and the energy gap of the GaAs substrate from the band gap of HfTiO film, as expressed

Journal of Materials Chemistry C Accepted Manuscript

in the following equation:

$$\Delta E_c(\text{HfTiO–InGaAs}) = E_g(\text{HfTiO}) - \Delta E_v(\text{HfTiO–GaAs}) - E_g(\text{GaAs}) \quad (2)$$

Where ΔE_c(HfTiO–GaAs) is the conduction band offset, E_g(HfTiO) is the band gap of HfTiO, ΔE_v(HfTiO–GaAs) is the valence band offset, and E_g(GaAs) is the band gap of GaAs substrate. By combining the band gap values and the VB lineup, the conduction band barrier height of the heterostructure can be determined. The extracted conduction band offset of the high-k films on GaAs is 0.79 eV, and 1.08 eV for the HfTiO and HfTiON films, respectively. Increase in conduction band offset has been detected after nitrogen incorporation, which is consistent with the previously reported result demonstrated on Si substrate.[21] Based on some reported results, it can be noted that the nitrogen concentration should be carefully controlled to guarantee excellent properties of HfTiON high-*k* dielectrics.[27] Some more work is under way to investigate the effect of nitrogen concentration on the band offset and electrical properties of HfTiON/GaAs gate satck. Fig. 9(b) and 9(c) summarize the nitrogen incorporation dependent energy-band alignment for HfTiON/GaAs gate stacks. Based on our observation, it can be deduced that the incorporation of N into HfTiO films leads to the reduction of valence band offset and increase in conduction band offset. Therefore, it can be concluded that energy-band diagrams in HfTiON films depend on the nitrogen content and can be modulated accurately, which is in good agreement with our previous observation.[21] For most high-*k* gate dielectrics, the asymmetric band alignments relative to channel materials results in larger leakage current.[41] In current study, the sputtering-derived HfTiON gate dielectric leads to near-symmetric band alignment and contributes to the increased electrical performance, which will be discussed later.

Based on the theoretical observation by Robertson that the band offset of high-k/high mobility substrate can be increased due to the existence of interfacial layer,[42] more attention has

Journal of Materials Chemistry C Accepted Manuscript

been paid to the investigation of angle-dependent valence band alignment of the HfTiON/GaAs gate stack with/without nitridation has been performed, as shown in Fig. 10. Based on Fig. 10(b), it can be noted that no obvious change in shape of the valence band spectra has been observed regardless of the probing depth, suggesting that no interface reaction happens and the interface chemical states and electronic structure of HfTiON/GaAs interface remains constant. However, for HfTiO/GaAs gate stack, with the increase of the emission angle, the valence band offset demonstrates an apparent increase, which originates from the existence of the oxide layer. As we know, with the increase in emission angle, the probing depth is close to the surface region. The increase in valence band offset indicates more formation of interfacial oxide layer, which agrees with previous ARXPS 2D images. According to analysis from band offset, it can be concluded that the band offset of HfTiO/GaAs gate stacks with nitridation is adequate for the gate dielectric operation with energy barriers over 1 eV.

Fig. 11(a) shows typical high frequency *C-V* characteristics of HfTiO and HfTiON gate dielectric MOS capacitors. Compared to HfTiON, HfTiO samples annealed at 500°C and 600°C exhibits decreased accumulation capacitance, which can be attributed to the high density of defective states at the conduction-band edge of GaAs caused by a considerable amount of As-O, As-As, and Ga-O bonds at the GaAs/HfTiON interface.[13,43] In addition, the hysteresis voltage almost disappears for HfTiON/GaAs samples annealed at different temperatures. Based on references, it can be noted that the hysteresis is due to the difference in gate bias at which electrons fill the traps and escape from the traps, or the difference between the capture and emission times of the border traps. As a result, the border traps increases with the oxygen content of the dielectric. Oxygen in HfTiO can easily diffuse to the interface, and thus traps (oxygen vacancies) are created in the dielectric. However, the nitrogen atoms can occupy these oxygen

Journal of Materials Chemistry C Accepted Manuscript

vacancies or form bonds with interstitial oxygen, and thus the nitrided samples have less oxygen-related traps and lead to the disappearance in hystersis.[26] The larger accumulation capacitance for the HfTiON sample annealed at 600°C than that annealed at 500°C is because better interface quality can be obtained at higher annealing temperature. The quasi-saturation of the *C-V* curve in the accumulation regime and a large slope in the depletion regime for the HfTiON sample annealed at 600°C indicate unpinned Fermi level and good interface properties.

In addition, the positive shift of flat band voltage (V_{fb}) indicates presence of negative oxide charges in the dielectric film. Compared to HfTiO, the HfTiON sample demonstrates smaller positive flat band voltage (V_{fb}) shift, indicating the lesst negative oxide charges, which can be attributed to either singly and doubly negatively charged interstitial oxygen atoms.[26] Based on Fig. 11, it can be noted that smaller positive shift of V_{fb} for the HfTiON sample annealed at 600°C than that annealed at 500°C should be due to the fact that more incorporated nitrogen atoms can diffuse to fill up the oxygen vacancies in the oxynitride during the higher annealing temperature, resulting in a reduction of defect traps in the film and near the interface.[22] The equivalent k value, V_{fb}, and oxide-charge density (Q_{ox}) of the HfTiO and HfTiON samples were extracted from HF *C-V* curves, as listed in Table 1. The oxide-charge density (Q_{ox}), including fixed charges, bordertrap charges, mobile-ion charges, and interface-state charges, is calculated according to $(Q_{ox})=-C_{ox}(V_{fb}-Ø_{ms})/q$, where $Ø_{ms}$ is the work-function difference between Au and GaAs substrate; C_{ox} is oxide capacitance per unit area.[44] Interface-state density (D_{it}) at midgap is also extracted from the *C-V* curves using the Terman's method for comparison purpose.[45] Due to the suppressed growth of the low-k interfacial layer, HfTiON/GaAs achieves the larger equivalent k value of 25.8. The negative Q_{ox} could be associated with acceptor-like interface and near-interface traps.[22,46] The Q_{ox} in HfTiON/GaAs sample is smaller than that of HfTiO/GaAs,

Journal of Materials Chemistry C Accepted Manuscript

probably due to the formation of more densified high-quality HfTiON films and better quality for the HfTiON/GaAs interfaces. Moreover, HfTiON/GaAs sample exhibit smaller D_{it} than that of HfTiO/GaA. This further indicates the effective blocking role of the HfON layer against the diffusions of Hf, Ti, and O towards the GaAs surface, as confirmed by previous XPS analysis, thus reducing the defects at/near the interface.[22] Based on the plot of leakage current density via gate voltage, shown in insert of Fig. 11(b), suppressed leakage current characteristics by applying nitride HfTiO gate dielectrics has been detected. The larger leakage current in HfTiO/GaAs sample is likely due to interface trap-assisted tunneling because a high density of interface states exists at the high-k/GaAs interface of the unpassivated samples.[47] However, a large reduction in gate leakage current density is obtained for the HfTiON samples, with 7.3×10^{-5} A/cm^2 and 3.6×10^{-4} A/cm^2 for the samples annealed at 600°C and 500°C, respectively. The smallest gate leakage current of the HfTiON sample annealed at 600°C is closely related to its smallest D_{it} and Q_{ox}. According to XPS analysis, it can be concluded that nitridation effectively protects against the oxidation of the substrate, suppresses the interfacial layer re-growth, and thus leads to the larger accumulation capacitance, the reduced oxygen-vacancies-related interface states, or the increased conduction band offset, leading to the reduced trap-assisted tunneling current.[20]

Fig. 12(a) and 12(b) show the *C-V* characteristics of MOS capacitors with HfTiO and HfTiON gate dielectric for a range of measurement frequencies between 1MHz and 1KHz. The dielectrics have received a PDA at 400 for 20s using RTA in N_2. The frequency dispersion of the accumulation capacitance is more prominent for capacitors with HfTiO dielectric. This dispersion is attributed to a high interface state density and associated Fermi level pinning.[48]

Journal of Materials Chemistry C Accepted Manuscript

Because of a large band gap of GaAs, the mid-gap states in the GaAs band gap cannot be assessed by *C-V* measurements between 1 MHz and 1 KHz at room temperature, the *C-V* characteristics have been carried out at a temperature of 150°C. At a higher temperature, the capture time constant of the mid-gap states is reduced or the characteristic frequencies of these mid-gap states is increased allowing the typical range of measurement frequencies between 1 MHz and 1 KHz to access the mid-gap states.[49] In Fig. 12, the bumps in the *C-V* curves in the depletion region are due to the presence of mid-gap states and high mid-gap interface state density. The D_{it} problem is more severe for HfTiO/GaAs gate stack than that of HfTiON/GaAs. Presence of interfacial Ga_2O_3 and As_2O_3 for HfTiO/GaAs gate stack creates defect levels close to the conduction band and the associated high trap density severely and contributes to the much larger frequency dispersion and stretch-out in *C-V* characteristics.

CONCLUSIONS

In summary, nitrogen composition dependent interface chemical bonding states, optical dielectric function, band alignment, and electrical properties of HfTiO/GaAs gate stacks grown by cosputtering have been investigated by ARXPS, SE, and electrical measurements. XPS analysis has confirmed that the interfacial layer of HfTiO/GaAs gate stack has been suppressed effectively after nitrogen incorporation. By means of SE measurements, reduction in band gap and increase in refractive index has been observed with the incorporation of nitrogen. Reduction in valence band offset and increase in conduction band offset have been observed for HfTiON/GaAs gate stack. As a result, improved *C-V* characteristics and reduced leakage current have been achieved from MOS capacitors of Au/HfTiON/GaAs/Al stack annealed at 600°C, which can be attributed to the removal of the defective interfacial oxides bonds, reduction in

Journal of Materials Chemistry C Accepted Manuscript

oxygen-related traps, and the enhanced barrier for the electron conduction by the Fermi level unpinning.

Acknowledgements

This work was supported by Anhui Provincial Natural Science Foundation (1208085MF99), Provincial Natural Science Foundation of Anhui Higher Education Institution of China (KJ2012A023), National Natural Science Foundation of China (No. 11104269, 51272001), Key Project of Chinese Ministry of Education (212082), Outstanding Young Scientific Foundation and Youth Science Research Foundation of Anhui University (KJJQ1103), and “211 project” of Anhui University.

Journal of Materials Chemistry C Accepted Manuscript

REFERENCES

1. T. Hoshii, S. H. Lee, R. Suzuki, N. Taoka, M. Yokoyama, H. Yamada, M. Hta, T. Yasuda, M. Takenaka, and S. Takagi, *J. Appl. Phys.*, 2012, 112, 073702.
2. S. Y. Lee, H. K. Kim, J. H. Lee, I. H. Yu, J. H. Lee, and C. S. Hwang, *J. Mater. Chem. C.*, 2014, 2, 2558.
3. C. Mahata, Y. C. Byun, C. H. An, S. Choi, Y. An, and H. Kim, *ACS Appl. Mater. Interfaces.*, 2013, 5, 4195.
4. D. Shahrjerdi, D. I. Garcia-Gutierrrez, E. Tatuc, and S. K. Banerjee, *Appl. Phys. Lett.*, 2008, 92, 223501.
5. G. He, X. S. Chen, J. G. Lv, H. S. Chen, B. Deng, and Z. Q. Sun, *Sci. Adv Mater.*, 2013, 5, 1410.
6. G. He, B. Deng, H. S. Chen, X. S. Chen, J. G. Lv, Y. Q. Ma, and Z. Q. Sun, *APL Mater.*, 2013, 1, 012104.
7. H. L. Lu, X. L. Wang, M. Sugiyama, and Y. Shimogaki, *Appl. Phys. Lett.*, 2009, 95, 212102.
8. J. Robertson, *Appl. Phys. Lett.*, 2009, 94, 152104.
9. C. L. Hinkle, M. Milojevic, B. Brennan, A. M. Sonnet, F. S. Aguirre-Tostado, G. J. Hughes, E. M. Vogel, and R. M. Wallace, *Appl. Phys. Lett.*, 2009, 94, 162101.
10. G. He, L. D. Zhang, M. Liu, and Z. Q. Sun, *Appl. Phys. Lett.*, 2010, 97, 062908.
11. G. He, L. D. Zhang, and M. Liu, *Appl. Phys. Lett.*, 2009, 95, 112905.

Journal of Materials Chemistry C Accepted Manuscript

12. S. Koveshnikov, W. Tasi, I. Ok, J. C. Lee, V. Torkanov, M. Yakimov, and S. Oktyabrsky, *Appl. Phys. Lett*., 2006, 88, 022106.
13. H. L. Lu, L. Sun, S. J. Ding, M. Xu, D. W. Zhang, and L. K. Wang, *Appl. Phys. Lett*., 2006, 89, 152910.
14. G. K. Dalapati, C. K. Chia, C. C. Tan, H. R. Tan, S. Y. Chiam, J. R. Dong, A. Das, S. Chattopadhyay, C. Mahata, C. K. Maiti, and D. Z. Chi, *ACS Appl. Mater. Interfaces*., 2013, 5, 949.
15. T. Moriizumi, and K. Takahashi, *Jpn. J. Appl. Phys*., 1969, 8, 348.
16. H. C. Lin, W. E. Wang, G. Brammertz, M. Meuris, and M. Heyns, *Microelectr. Eng*., 2009, 86, 1554.
17. H. Zhao, J. H. Yum, Y. T. Chen, and J. C. Lee, *J. Vac. Sci. Technol. B* 2009, 27, 2024.
18. Y. S. Kang, D. K. Kim, K. S. Jeong, M. H. Cho, C. Y. Kim, K. B. Chung, and D. C. Kim, *ACS Appl. Mater. Interfaces*., 2013, 5, 1982.
19. G. He, X. S. Chen, and Z. Q. Sun, *Sur. Sci. Rep*., 2013, 68, 68.
20. M. Seo, S. K. Kim, Y. S. Min, and C. S. Hwang, *J. Mater. Chem*., 2011, 21, 18497.
21. G. He, Z. Q. Sun, Y. Q. Ma, M. Z. Wu, Y. M. Liu, S. W. Shi, G. Li, X. S. Chen, L. D. Zhang, Z. B. Fang, *Semi. Sci. Tech*., 2011, 26, 105019.
22. L. S. Wang, J. P. Xu, S. Y. Zhu, and P. T. Lai, *Appl. Phys. Lett*., 2013, 103, 092901.
23. X. Wang, X. Q. Cao, L. Bourgeois, H. Guan, S. M. Chen, Y. T. Zhong, D. M. Tang, H. Q. Li, T. Y. Zhai, L. Li, Y. Bando, and D. Golberg, *Adv. Func. Mater*., 2012, 22, 2682.
24. X. Wang, Q. H. Weng, X. Z. Liu, X. B. Wang, D. M. Tang, W. Tian, C. Zhang, D. Q. Liu, Y. Bando, D. Golberg, *Nano Let*t., 2014, 14, 1164.
25. F. Ji, J. P. Xu, P. T. Lai, C. X. Li, and J. G. Guan, *Appl. Phys. Lett*., 2007, 91, 052902.

Journal of Materials Chemistry C Accepted Manuscript

Journal of Materials Chemistry C Accepted Manuscript

26. L. M. Lin, and P. T. Lai, *J. Mater. Sci.: Mater. Electron*., 2008, 19, 894.

27. M. Liu, X. J. Wang, Y. Y. Luo, H. M. Wang, S. H. Kang, L. D. Zhang, and Q. Fang, *J. Appl. Phys*., 2011, 110, 024110.

28. H. S. Kim, I. Ok, M. Zhang, C. Choi, T. Lee, F. Zhu, G. Thareja, L. Yu, and J. C. Lee, *Appl. Phys. Lett*., 2006, 88, 252906.

29. G. He, G. W. Meng, L. D. Zhang, and M. Liu, *Appl. Phys. Lett*., 2007, 91, 232910.

30. Y. Baba, T. A. Sasaki, and I. Takano, *J. Vac. Sci. Technol. A* 1988, 6, 2945.

31. G. He, M. Liu, L. Q. Zhu, M. Chang, Q. Fang, and L. D. Zhang, *Surf. Sci*., 2005, 576, 67.

32. C. Ye. H. Wang, J. Zhang, Y. Ye, Y. Wang, B. Y. Wang, and Y. C. Jin, *J. Appl. Phys*., 2010, 107, 104103.

33. G. He, Q. Fang, G. H. Li, and L. D. Zhang, *J. Phys. D: Appl. Phys*., 2008, 41, 045304.

34. C. V. Ramana, G. Baghmar, E. J. Rubio, and M. J. Hernandez, *ACS Appl. Mater. Interfaces*., 2013, 5, 4659.

35. G. He, L. D. Zhang, G. H. Li, M. Liu, L. Q. Zhu, S. S. Pan, and Q. Fang, *Appl. Phys. Lett*., 2005, 86, 232901.

36. D. Mergel, D. Buschendorf, S. Eggert, R. Grammes, and B. Samset, *Thin Solid Films*. 2000, 371, 218.

37. G. He, L. D. Zhang, G. W. Meng, G. H. Li, G. T. Fei, X. J. Wang, J. P. Zhang, M. Liu, Q. Fang, and I. W. Boyd. *J. Appl. Phys*. 2008, 104, 104116.

38. X. J. Wang, L. D. Zhang, M. Liu, J. P. Zhang, and G. He, *Appl. Phys. Lett*., 2008, 92, 122901.

39. E. A. Kraut, R. W. Grant, J. R. Waldrop, and S. P. Kowalczyk, *Phys. Rev. Lett*., 1980, 44, 1620.

40. H. Y. Yu, M. F. Li, B. J. Cho, C. C. Yeo, M. S. Joo, D. L. Kwong, J. S. Pan, C. H. Ang, J. Z.

Zheng, and S. Ramanathan, *Appl. Phys. Lett*., 2002, 81, 376.

41. H. J. Osten, J. P. Liu, and H. J. Mussing, *Appl. Phys. Lett*., 2000, 80, 297.
42. J. Robertson, and B. Falabretti, *J. Appl. Phys*., 2006, 100, 014111.
43. T. Yang, Y. Xuan, D. Zemlyanov, T. Shen, Y. Q. Wu, J. M. Woodall, P. D. Ye, F. S. Aguirre-Tostado, M. Milojevic, S. McDonnell, and R. M. Wallace, *Appl. Phys. Lett*., 2007, 91, 142122.
44. J. P. Xu, F. Ji, C. X. Li, P. T. Lai, J. G. Guan, Y. R, Liu, *Appl. Phys. Lett*., 2007, 91, 152905.
45. R. Engel-Herbert, Y. Hwang, and S. Stemmer, *J. Appl. Phys*., 2010, 108, 124101.
46. F. Ji, J. P. Xu, P. T. Lai, C. X. Li, and J. G. Liu, *IEEE Electron Device Lett*., 2011, 32, 122.
47. F. Gao, S. J. Lee, D. Z. Chi, S. Balakumar, and D. L. Kwong, *Appl. Phys. Lett*., 2007, 90, 252904.
48. C. L. Hinkle, M. Milojevic, B. Brennan, A. M. Sonnet, F. S. Aguirre-Tostado, G. J. Hughes, E. M. Vogel, and R. M. Wallace, *Appl. Phys. Lett*., 2009, 94, 162101.
49. G. Brammertz, H. C. Lin, K. Martens, D. Mercier, S. Sioncke, A. Delabie, W. E. Wang, M. Caymax, M. Meuris, and M. Heyns, *Appl. Phys. Lett*., 2008, 93, 183504.

Journal of Materials Chemistry C Accepted Manuscript

Figure Captions

Fig.1. Nitrogen dependent Hf 4*f* (a) and Ti 2*p* (b) XPS spectra of HfTiO/GaAs gate stacks.

Fig.2. (a) and (b) Nitrogen dependent Ti 2*p* XPS spectra of HfTiO/GaAs gate stacks.

Fig.3. (a) and (b) Nitrogen dependent As 3*d* XPS spectra of HfTiO/GaAs gate stacks

Fig.4. (a) and (b) Nitrogen dependent O 1*s* XPS spectra of HfTiO/GaAs gate stacks

Fig.5 ARXPS 2D images of As 3*d* (a), Hf 4*f* (b), O 1*s* (c), and Ti 2*p* (d) XPS spectra of HfTiON/GaAs gate stacks

Fig.6. ARXPS 2D images of As 3*d* (a), Hf 4*f* (b), O 1*s* (c), and Ti 2*p* (d) XPS spectra of HfTiO/GaAs gate stacks

Fig.7.The experimental (open circles) and fitted (solid lines) spectroscopic ellipsometric data for HfTiO (a) and HfTiON (b) samples.

Fig.8. (a) The optical constants of HfTiO and HfTiON film. The inset in (a) shows the determination of the band gap of HfTiO and HfTiON film. (b) The nitrogen content dependent real part (ε_1) of the dielectric functions of HfTiO films. The inset in (b) shows the nitrogen dependent imaginary part of (ε_2) part the dielectric functions of HfTiO films.

Fig.9. (a) Detailed valence-band spectra of HfTiO and HfTiON dielectrics on GaAs substrate. Schematic energy band alignment of HfTiO/GaAs (b) and HfTiO/GaAs (c) gate stack.

Fig.10. (a) and (b) Angular-dependent valence band spectra of HfTiO/GaAs gate stacks with/without nitridation.

Journal of Materials Chemistry C Accepted Manuscript

Fig.11. *C-V* (a) and *J-V* (b) characteristics of GaAs-based MOS capacitors with and without nitrogen incorporation.

Fig. 12 Frequency dependent *C-V* characteristics of GaAs MOS capacitors with HfTiO (a) and HfTiON layer (b).

TABLE I. Parameters of the GaAs MOS capacitors extracted from HF *C-V* curves.

Journal of Materials Chemistry C Accepted Manuscript

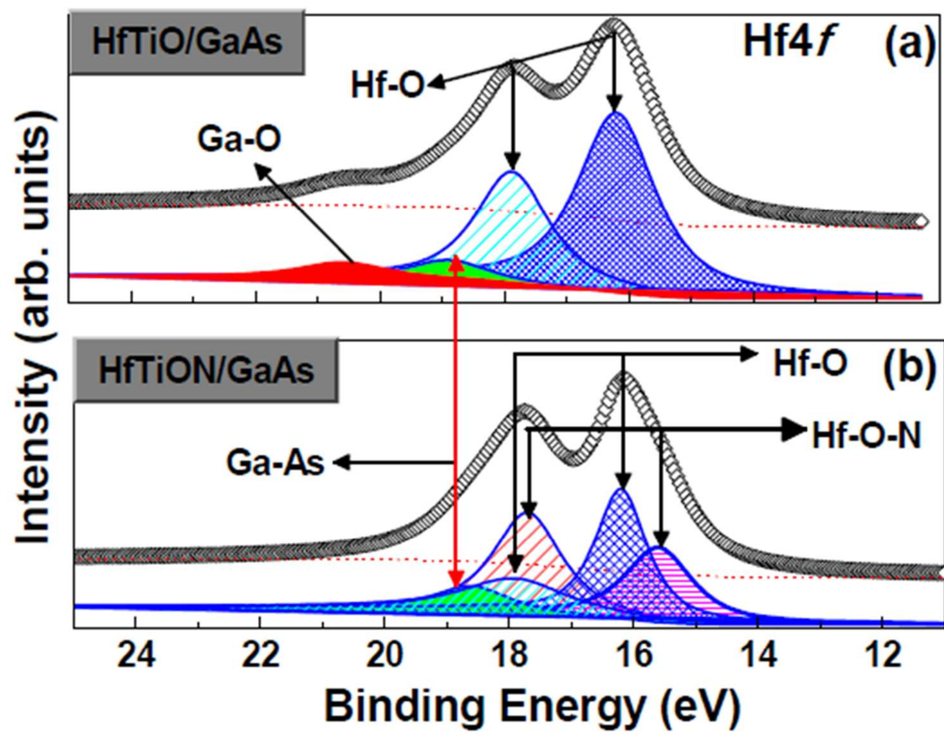

Fig.1. He *et al.*

Journal of Materials Chemistry C Accepted Manuscript

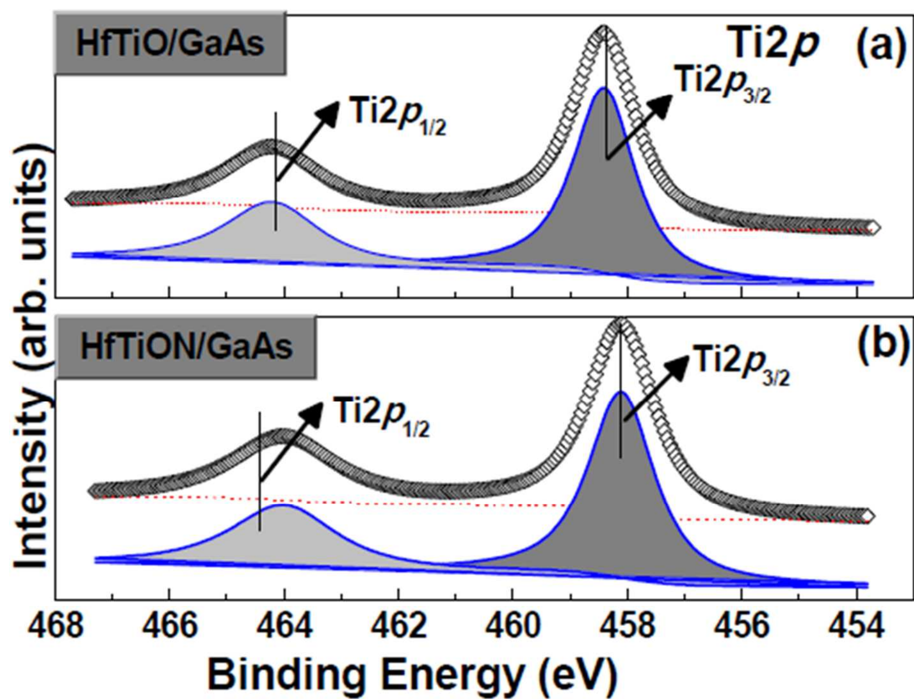

Fig.2. He *et al.*

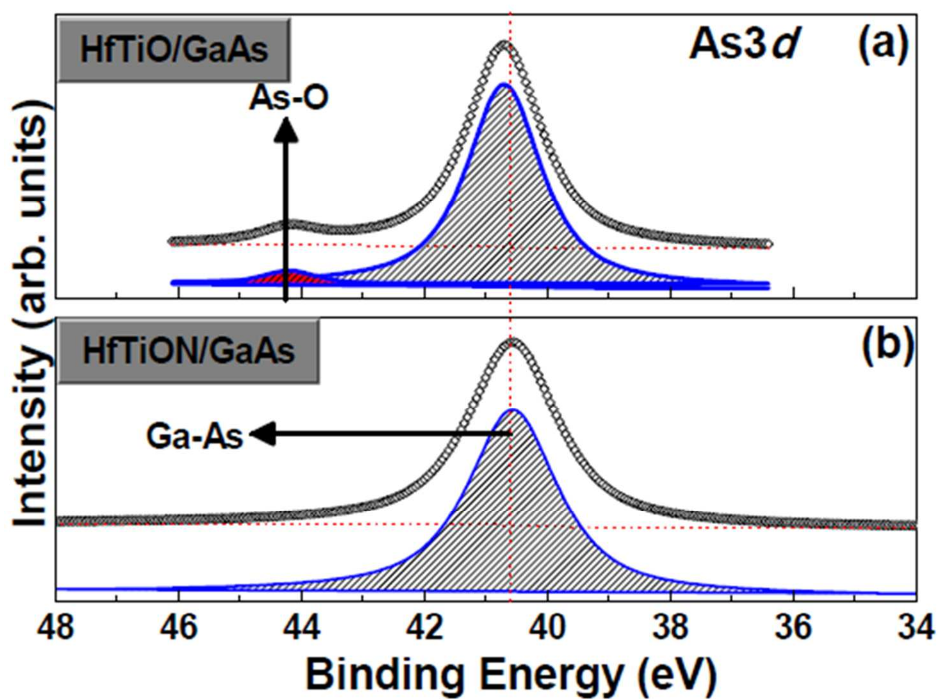

Fig.3. He et al.

Journal of Materials Chemistry C Accepted Manuscript

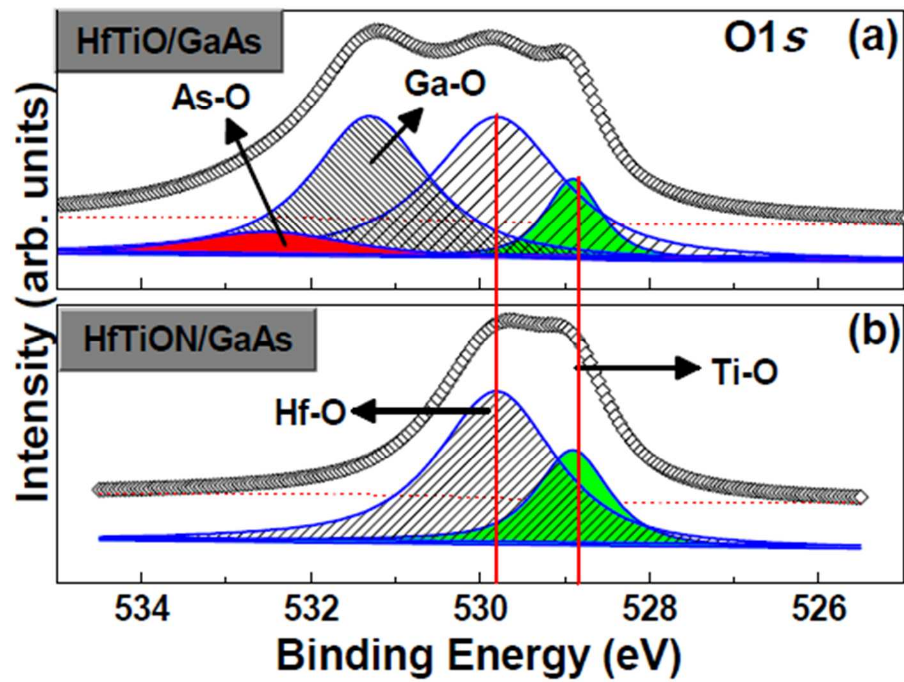

Fig.4. He *et al.*

Journal of Materials Chemistry C Accepted Manuscript

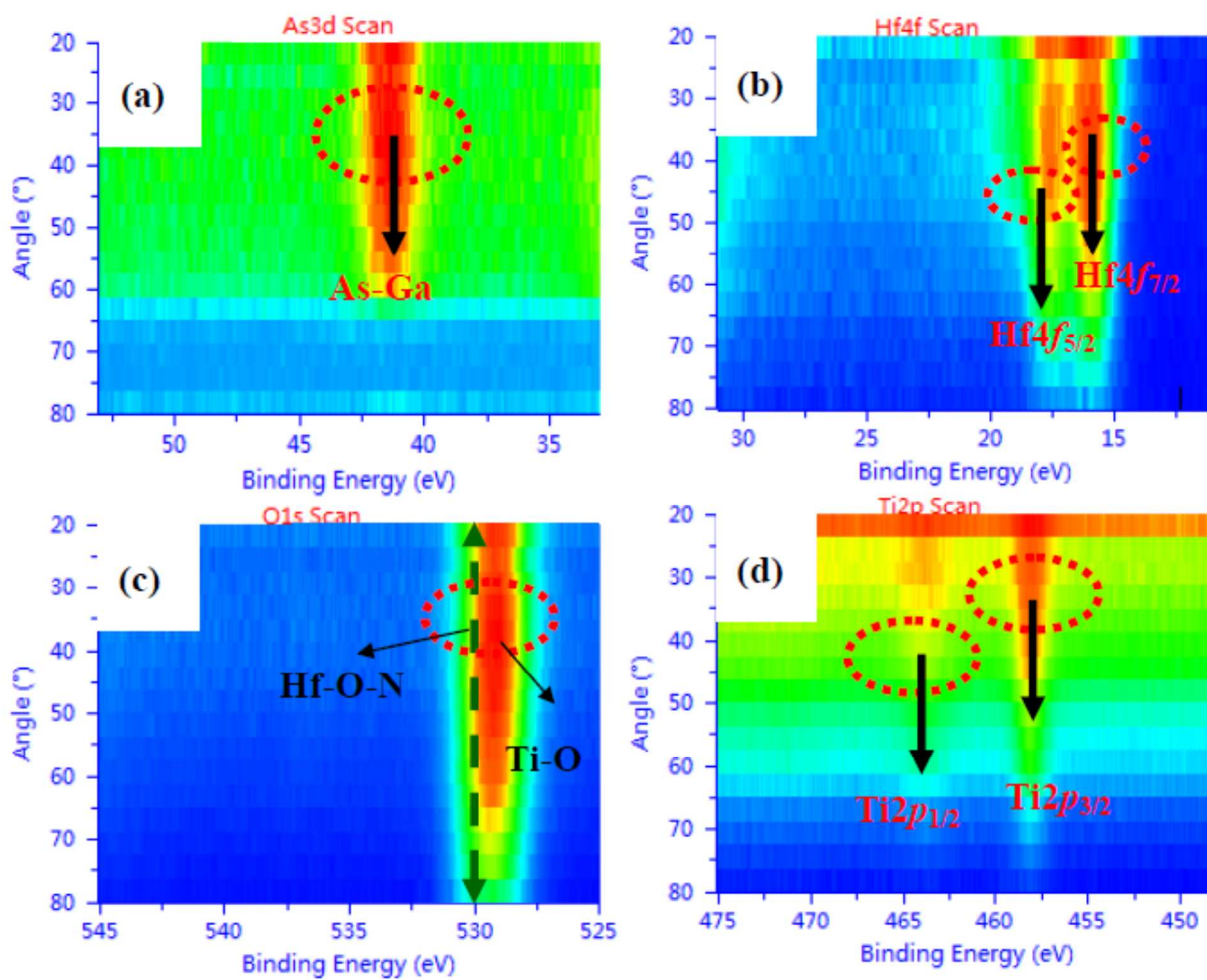

Fig.5. He *et al.*

Journal of Materials Chemistry C Accepted Manuscript

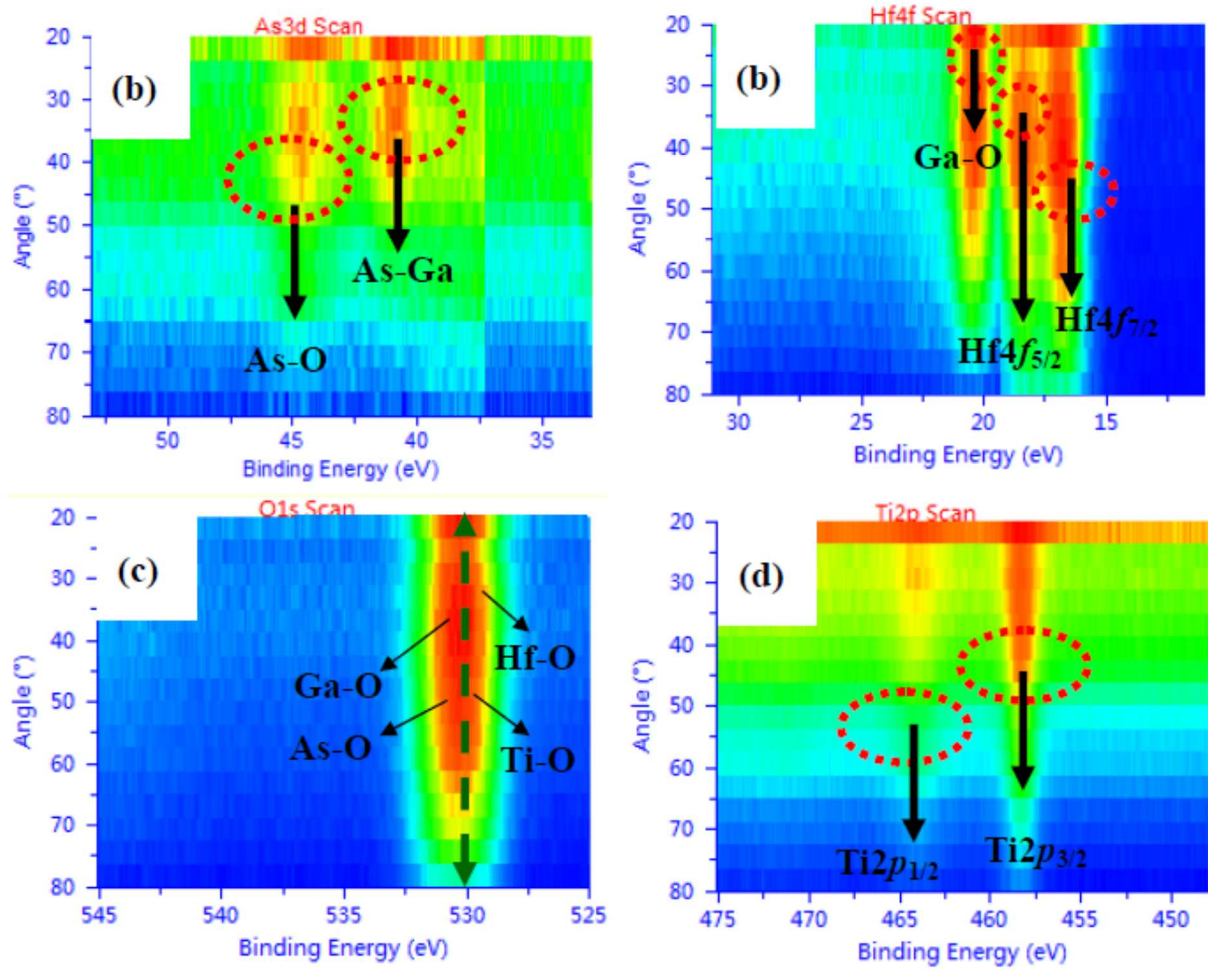

Fig.6. He *et al.*

Journal of Materials Chemistry C Accepted Manuscript

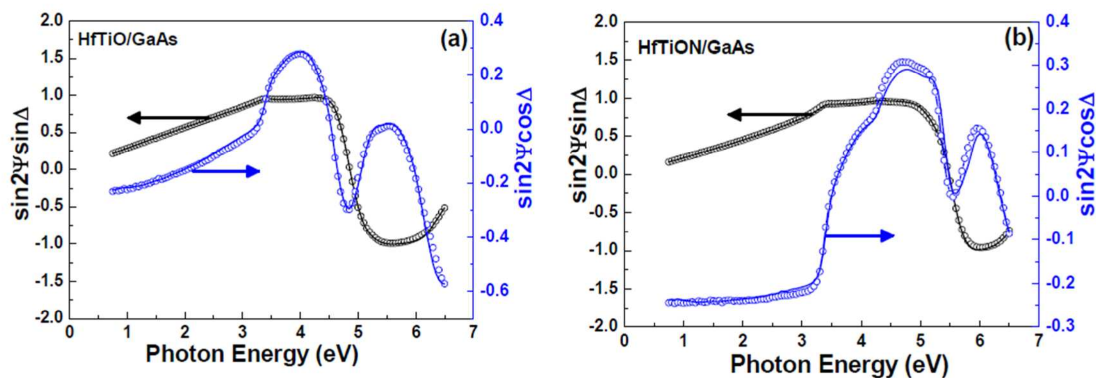

Fig.7. He *et al.*

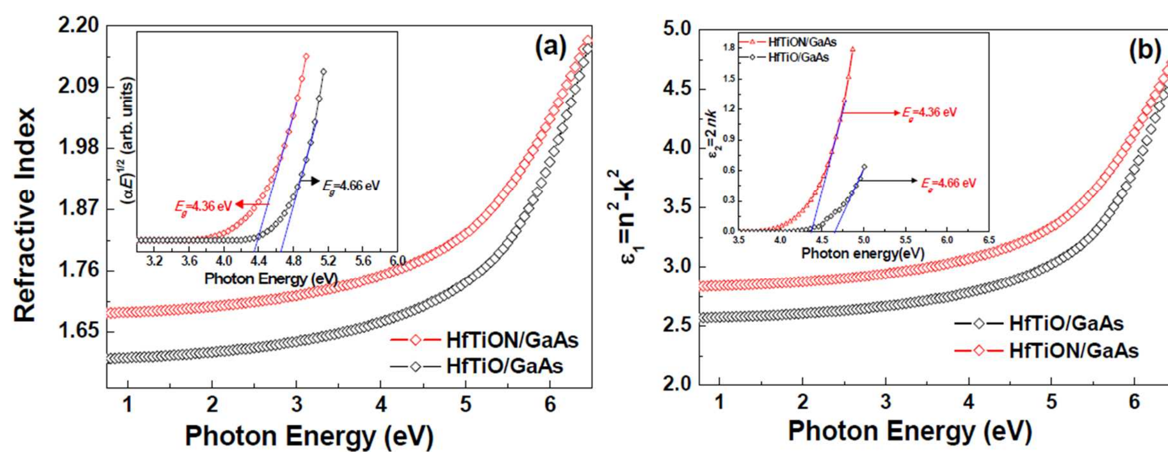

Fig.8. He *et al.*

Journal of Materials Chemistry C Accepted Manuscript

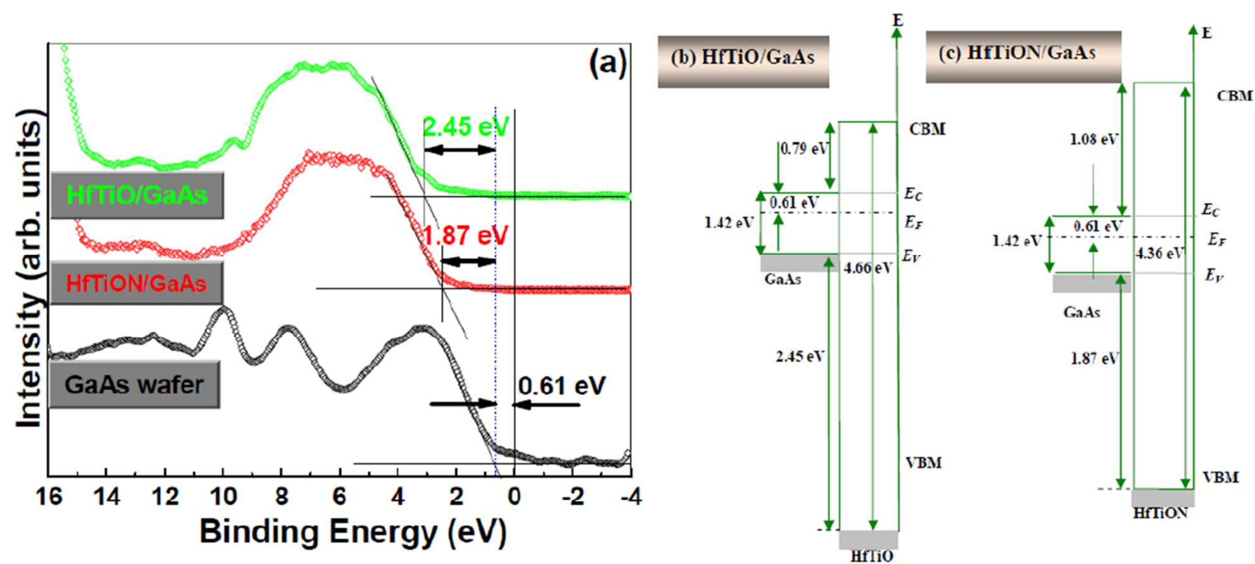

Fig.9. He *et al.*

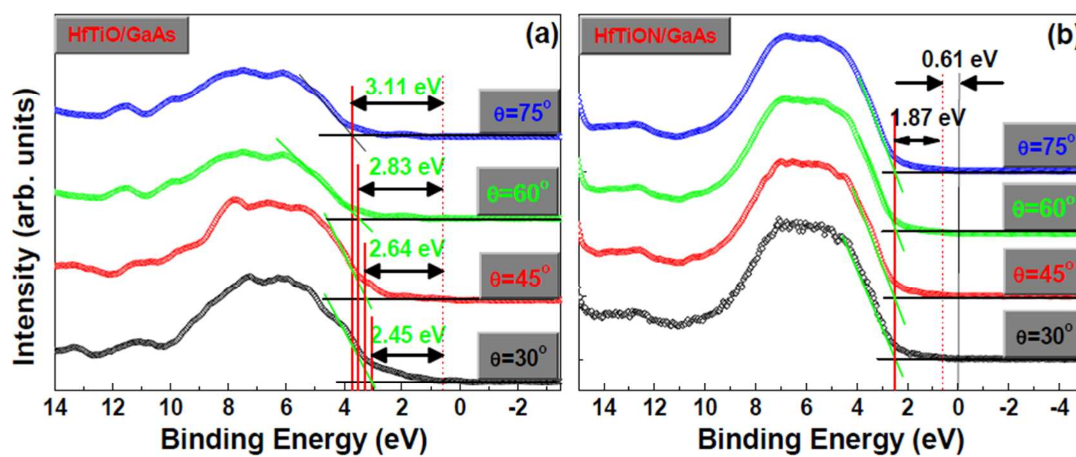

Fig.10. He *et al.*

Journal of Materials Chemistry C Accepted Manuscript

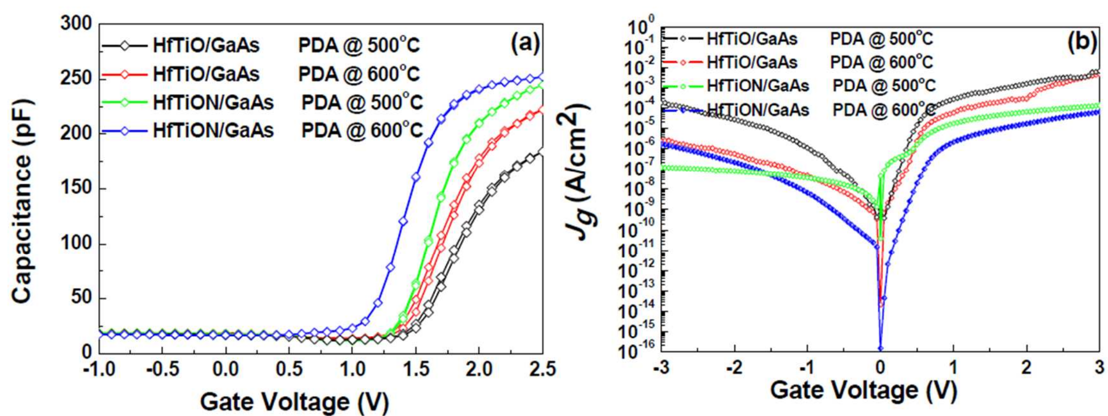

Fig.11. He *et al.*

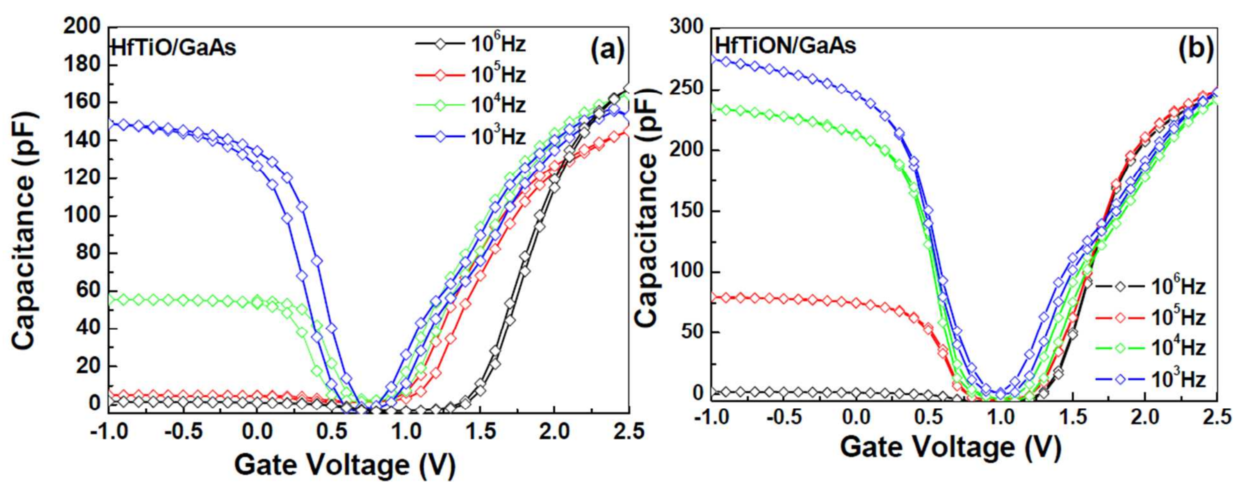

Fig.12. He *et al.*

Journal of Materials Chemistry C Accepted Manuscript

Sample	V_{fb} (V)	Q_{ox} (cm^{-2})	D_{it} ($cm^{-2}ev^{-1}$)	k
HfTiO/GaAs 600°C	1.69	-2.5×10^{13}	8.3×10^{12}	20.5
HfTiO/GaAs 500°C	1.78	-5.6×10^{13}	9.5×10^{12}	19.6
HfTiON/GaAs 600°C	1.29	-7.6×10^{12}	2.8×10^{12}	25.8
HfTiON/GaAs 500°C	1.65	-8.5×10^{12}	3.2×10^{12}	24.7

Table. 1 He *et al.*

Journal of Materials Chemistry C Accepted Manuscript